Numerical Simulation Study of the Mori Geothermal Field, Japan

Kazuyoshi Osada[1], Mineyuki Hanano[2], Kei Sato[1], Tatsuya Kajiwara[1], Fumiaki Arai[1], Masato Watanabe[1], Seiji Sasaki[3], Osamu Sako[3], Yoshinobu Matsumoto[4] and Shouji Yamazaki[4]

[1.]JMC Geothermal Engineering Co., Ltd., 356-6 Oshimizu, Ogama, Takizawa-mura, Iwate 020-0151 Japan

[2.]Japan Metals and Chemicals Co., Ltd., 1-17-25 Shinkawa, Chuo-ku, Tokyo 104-8257 Japan

[3.]Hokkaido Electric Power Co., Inc., 1-2 Odori-Higashi, Chuo-ku, Sapporo-shi, Hokkaido 060-8677 Japan

[4.]Hokkaido Power Engineering Co., Inc., 1-2-1 Kita 4-jo Nishi, Chuo-ku, Sapporo-shi, Hokkaido 060-0004 Japan

osada@geothermal.co.jp

Keywords: Simulation, natural state, history matching, prediction, Mori, geothermal, caldera, reservoir, well

ABSTRACT

A numerical simulation study of the Mori geothermal field was carried out to analyze and predict the behavior of the reservoir, production wells and re-injection wells. This study consisted of three-dimensional natural state modeling, history matching and future prediction. The numerical model provided satisfactory matches of temperature and pressure profiles in the natural state and of wells' temperature and pressure history during exploitation. Therefore the numerical model constructed in these simulations was thought to be able to reproduce the actual field conditions.

By using this numerical model, the total steam flow rate trends were predicted for several different scenarios over the next 10 years. The results indicate that the reservoir will be able to sustain stable total steam production by drilling new production wells and new re-injection wells. With the addition of these new re-injection wells, the flow rate of the existing re-injection well that have adverse effects on some of the existing production wells can be decreased.

1. INTRODUCTION

The Mori geothermal field is a liquid-dominated geothermal field located in the Nigorikawa caldera, which was formed about 12,000 years ago (Sumi and Takashima, 1975), in Hokkaido, Japan (Figure 1), and the Mori geothermal power station (50 MWe) has been in operation in the field since 1982. As shown in Figure 2, the geological setting of the reservoir consists of the Pre-Tertiary Kamiiso Group, the Neogene Ebiyagawa Formation that unconformably overlies the Kamiiso Group, and the Quaternary caldera fill deposits (e.g. Sato, 1988; Ando et al., 1992; Kurozumi and Doi, 2003). The fractures near the caldera wall, the margins of intrusions, and fractures confined to some lithofacies in the Kamiiso Group are recognized as high permeable zones (Akazawa et al., 1993).

Sakagawa et al. (1994) conducted an earlier three-dimensional numerical simulation of the Mori geothermal field, which included natural state and history matching and prediction of the reservoir behavior. Our study updated their numerical model in order to refine the model and the prediction runs. First we evaluated the accuracy of the numerical model based on the matching between measured and calculated parameters such as temperature and pressure for the natural state. Then we followed the histories of temperature and pressure during operation. Through this process, the model was modified and refined. Finally, the best model was used for prediction to find a development scenario that provides sustainable operation of the power station.

In this study we used the STAR reservoir simulator (Pritchett, 1995), which treats both porous and dual-porosity media. A porous model was used in natural state modeling, and a dual-porosity model was partially used in history matching and future prediction.
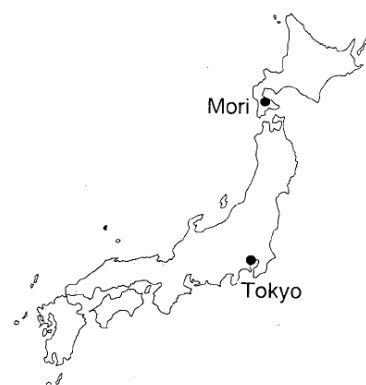

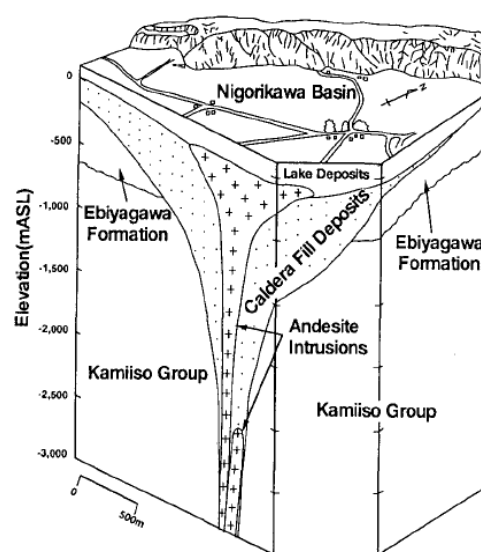Figure 1: Location of the Mori geothermal field.

Figure 2: Schematic geological setting of the reservoir of the Mori geothermal field (modified from Kurozumi and Doi, 2003）.

2. NUMERICAL MODEL

Our study revised the numerical model of Sakagawa et al. (1994), to incorporate the deeper production wells that were drilled after 1994 and in order to carry out the history matching including the data obtained after 1994.

2.1 Study Area and Grid Geometry

The horizontal study area was set to be 11,400 m along northeast-southwest and 11,300 m along northwest-southeast, and the vertical study area was set to be 5,200 m (Figure 3 and 4). The study area was divided into a 20 x 19 x 29 grid, and the minimum size of grid was 100 m x 100 m x 100 m. The reasons for deciding the vertical study area and grid size are described as follows.
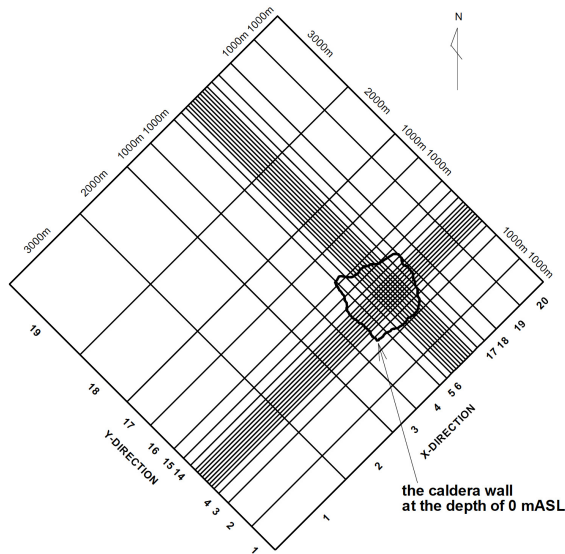
Figure 3: Horizontal study area and grid division.

In the first run of history matching, the calculated temperature of the deep production wells showed minimal decline with time after the start of exploitation, although the measured temperature showed a significant drop for the same period. We believed the reasons are as follows.

a) The grids involving the feed points of the deep production wells are adjacent or very close to the grids where recharge is set.

b) The size of grids involving feed points is too large; the minimum size is 200 m x 200 m x 100 m.

In order to represent up-flow of the deep hot recharge, constant rate mass input was imposed on some grids in the lower-most layer. Because of reason (a), high temperature fluid from the recharge grids was thought to flow into the grids involving the feed points directly. Thus the calculated temperature of feed points did not decrease as expected. In order to solve this problem and to incorporate the deeper wells that were drilled after 1994, the depths of the recharge grids (that is the depth of the lower-most layer) were set deeper. Thus, high temperature fluid from the recharge grids was prevented from flowing into the grids involving the feed points.

In order to solve the problem described in reason (b), the study area was divided into a finer grid. In doing so, the value of heat capacity of each grid becomes smaller, and the calculated fluid temperature of each grid can easily change. Also, in a dual-porosity model, the transference of

heat is fast because of the high permeability in fractures. As grids are smaller, the flow in the numerical model is closer to the actual flow. As shown in Figure 3, the area around the Nigorikawa caldera was divided into a finer grid.

2.2 Boundary Conditions

Pressures at the top boundary were set at different levels to account for the possible effect of elevation differences within the mountainous area around Nigorikawa caldera. The temperature of each upper-most grid was assigned based on the results of temperature logs in static wells and temperature distribution at one-meter deep from the ground reported by Urakami and Nishida (1977). All side boundaries were closed to conductive heat flow and mass flow.

The condition of the bottom boundary was set as follows: the recharge rate was set to be 27.5 kg/s with 280-340°C; the conductive heat flux was set to be 0.2 W/m^2 around caldera and 0.1 W/m^2 in the area except for the area set to be 0.2 W/m^2. The reasons are described below.

The distribution of recharge rate, the fluid temperature and the conductive heat flux were chosen to obtain good matches in the natural state modeling and the history matching. The maximum fluid temperature was set to be 340°C because the fluid temperature from the deep part was thought to be higher than the maximum value among the temperatures measured in static wells, which is about 330°C. The location of the recharge grids was set at X of 6 to 16 and Y of 5 to 12 (Figure 3).

The conductive heat flux around the caldera was set to be 0.2 W/m^2. In the remote area from the caldera, the conductive heat flux was set to be 0.1 W/m^2 because the heat flux was thought to be lower than around the caldera.

2.3 Initial Conditions

The initial temperature distribution for the natural state modeling is linear for depth and laterally uniform: 20°C at the surface and 340°C at the bottom. The initial pressure of each layer in the natural state is set to be hydrostatic with a uniform pressure distribution of 2.5 bars at the top surface (100 mASL).

2.4 Rock Properties

The natural state modeling was carried out with a porous media model. History matching and future prediction were carried out with a dual-porosity model for the high permeable areas. In the dual-porosity model, the rock properties of the fractures were set to be equal to those of the matrix except for the permeability.

Values of porosity, rock density, thermal conductivity, heat capacity of rock, and permeability used in the initial model were assigned to each geological structure element or lithofacies. The porosity, the rock density and thermal conductivity of rock were based on the core data. The heat capacity of rock was taken as 10^{30} J/kg K in the upper-most layer so that the temperature of the upper-most layer would be constant and 1,130 J/kg K in the other layers.

Permeability distribution was initially based on the rock types or geological information, i.e. the ground water aquifer, the caldera fill deposits, the Ebiyagawa Formation, the Kamiiso Group, the intrusions in and near the caldera, the shallower and deeper part of the caldera wall. The permeability values were then adjusted to obtain good
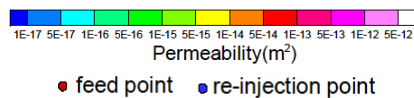
matches basically about the natural state modeling and the history matching (Figure 4).
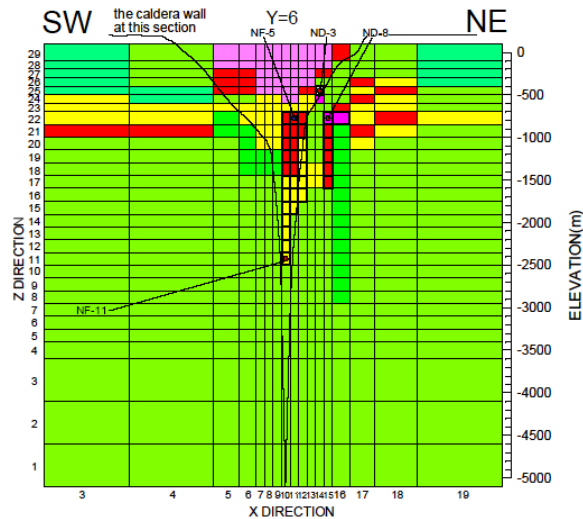
(a)   Horizontal permeability
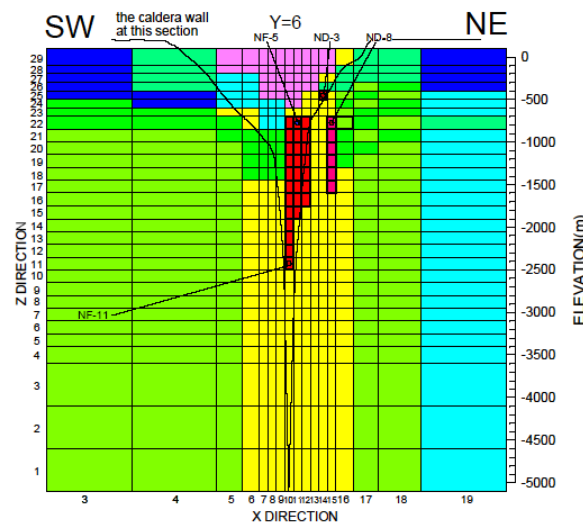

(b)   Vertical permeability

Figure 4: Permeability distribution in a dual-porosity model (The grids surrounded by bold lines are dual-porosity model; denoted by the permeability of fracture).

3.   RESULTS OF THE NATURAL STATE MODELING

The duration of the calculation was 15,000 years. At the end of the run, the flow of mass and heat approached steady state. Therefore the conditions obtained by the calculation were assumed to be those before the exploitation. The results of the natural state modeling were matched to temperature profiles and reservoir pressure measured in wells before the exploitation in the Mori geothermal field. Figure 5 shows some of the temperature matches for the best model. The figure shows good matches in general. Thus, the numerical model is thought to reproduce the mass and heat flow in the reservoir. Note that since the temperature in well ND-11 was measured after the start of

exploitation, the match is not good compared with that in other wells.

Figure 6 shows the match about the pressure distribution. The figure shows that the model reproduced well the pressure distribution. This result indicates that the average temperature and permeability of the whole study area is realistic enough. Thus, the amount of the mass input and the conductive heat flux imposed to the deepest part of study area and the pressure distribution imposed to the top boundary are reasonable.
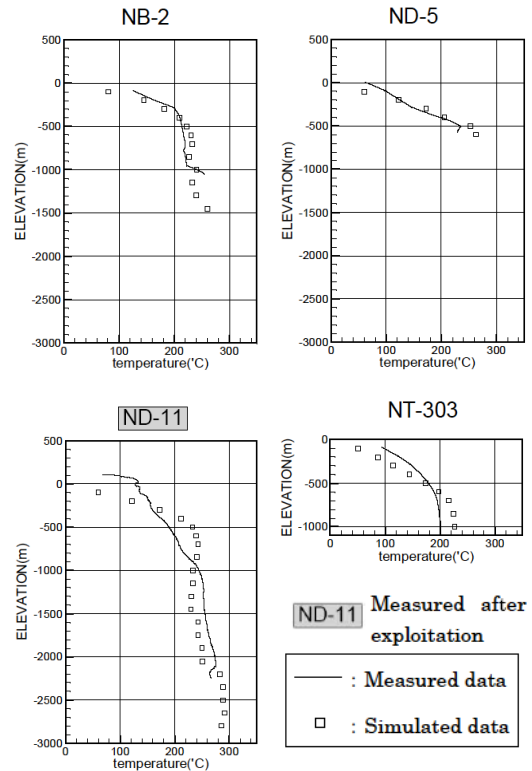
Figure 5: Some of the matches about the temperature profiles of wells in natural state modeling.
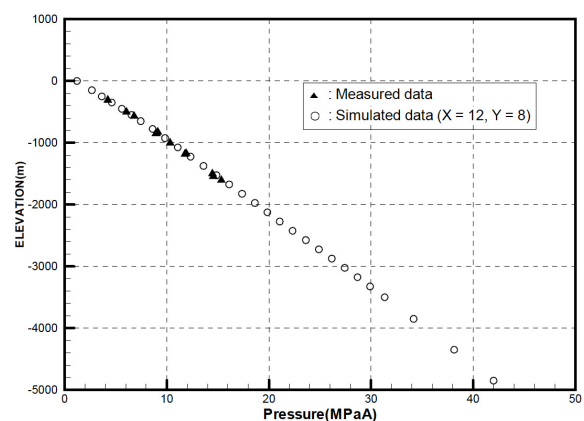
Figure 6: Match about the pressure distribution in natural state modeling.

Figure 7 shows the calculated temperature distribution in vertical section and mass vectors. The length of vectors is set to be constant. The figure shows that the geothermal fluid ascends around the caldera and flows laterally, and the shallow ground water is reserved in the shallow part of the caldera. This flow state is consistent with that of the current reservoir model (Hanano et al., 2005).
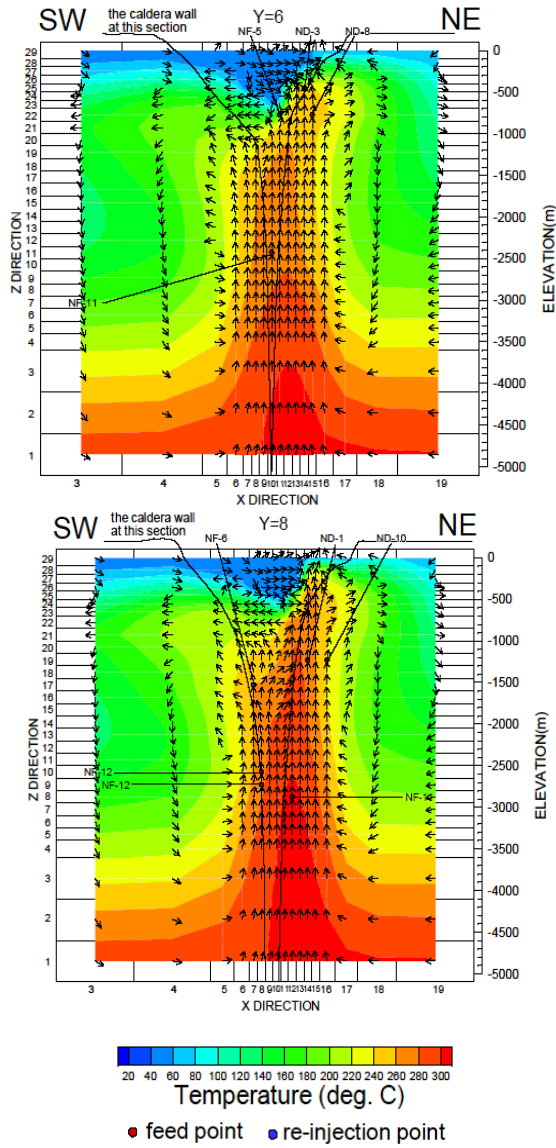
Osada et al.

Figure 7: Calculated temperature distribution (vertical section) and mass vectors in natural state modeling.

4. RESULTS OF THE HISTORY MATCHING

From the natural state, the study proceeded to obtaining good matches of temperature history at feed points of production wells and reservoir pressure history measured in observation wells. Figure 8 shows some of the matches about temperature history. Three sets of measured temperature were used for comparison with model data; the temperature calculated by the silica concentration of production fluid, the temperature logging in the production wells, and the temperature based on the tracer flow test (TFT). Figure 8 shows that the matches of the temperature history are good in general. However, poor matches were obtained, particularly the rate of temperature decline, for some of the production wells which were affected significantly by re-injection fluid (e.g. NF-1). For these wells, we opted to just reproduce the value and trend of the temperature at the later portion of history matching (which will become the initial condition for prediction runs).

Figure 9 shows some of the matches about pressure history. The figure shows that the matches of the pressure history are quite good.
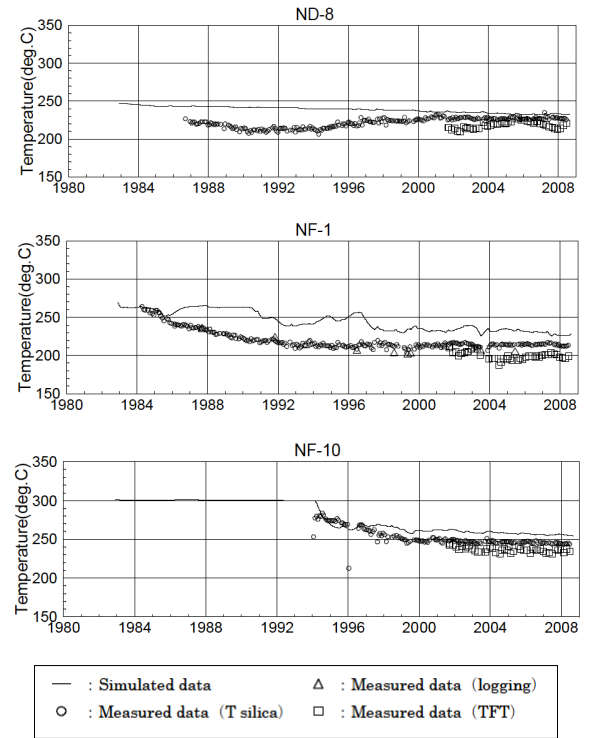

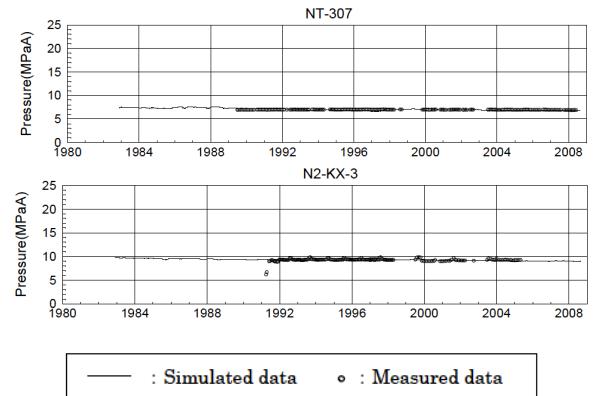**Figure 8: Some of the matches about temperature history.**

Figure 9: Some of the matches about pressure history.

5. RESULTS OF THE FUTURE PREDICTION

By using the numerical model obtained by the natural state modeling and history matching, the prediction run was carried out to model the resource behavior for the next 10 years. The details of scenarios of the prediction run are shown in Table.1.

i. In all scenarios new re-injection well Well-r1, Well-r2, and new production well Well-p1 are drilled. However, the new production well Well-p2 is drilled only in scenario08-*N*-2 (*N* =1-4). The re-injection points of Well-r1 and Well-r2 are distant from the caldera.

ii. According to the re-injection capacity of Well-r1 and Well-r2, the scenarios are classified mainly into three cases; Re-injection well NF-6 can be stopped (in the scenario08-1-*N* and 08-2-*N* ; *N* =1,2), NF-6 cannot be stopped however the flow rate of NF-6 can be decreased (in the scenario08-3-*N*), and the flow rate of NF-6 can not be changed (in the scenario08-4-*N*). The re-injection point of NF-6 is close to the caldera wall.

4

Table 1: Content of scenarios of the future prediction.

| Well-p2 (Production well) | | The change of re-injection rate of NF-6 due to re-injection rate of Well-r1 or Well-r2 | | | |
| | | 2010/7 | | 2011/9 | |
Not drilled	Drilled(2013/9)	Well-r1 (drilled)	Re-injection well NF-6	Well-r2 (drilled)	Re-injection well NF-6
scenario08-1-1	scenario08-1-2	100t/h	Stopped [100→0t/h]	90t/h	Under suspention
scenario08-2-1	scenario08-2-2	75t/h	100→60t/h	90t/h	Stopped [60→0t/h]
scenario08-3-1	scenario08-3-2	50t/h	Not changed [100t/h]	90t/h	90→60t/h
scenario08-4-1	scenario08-4-2	50t/h	Not changed [100t/h]	50t/h	Not changed [90t/h]

Figure 10 shows the result of prediction of steam flow rate. The power station was assumed to be under regular maintenance for periods of one or two months every year. For these periods, the production and re-injection were stopped. Figure 10 indicates the following:

i. In order to sustain the average steam flow rate of 200t/h in 2017-2018, re-injection to the caldera wall through NF-6 needs to be stopped and replaced with re-injection farther from the caldera through Well-r1 or Well-r2 (scneario08-1-2 and 08-2-2).

ii. Also in order to sustain 200t/h, it is necessary to drill Well-p2 (in the scenario08-1-2 and 08-2-2).

iii. If the re-injection capacity obtained by drilling Well-r1 or Well-r2 is not enough to replace NF-6, the average steam flow rate in 2017-2018 does not sustain 200t/h and is slightly under (in the scenario08-3-2 and 08-4-2).

iv. The case where Well-p2 is not drilled and NF-6 can be stopped is equivalent to the case where Well-p2 is drilled and NF-6 cannot be stopped (The results of scenario08-1-1 and 08-2-1 are similar to those of scenario08-3-2 and 08-4-2).
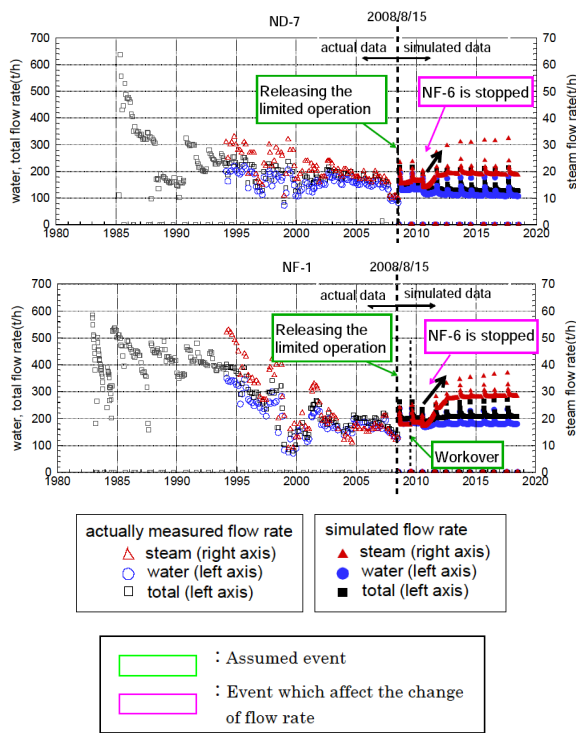
Figure 11 shows the results of prediction of production rate in well ND-7 and NF-1 in the scenario08-1-1, in which NF-6 can be stopped. The figure indicates that the steam flow rates in both wells increase sharply just after NF-6 is stopped (2010/7). These results support the idea that NF-6 has significant adverse effect on ND-7 and NF-1 as indicated by the results of tracer tests,. Because the steam flow rates in ND-7 and NF-1 will recover, the total steam flow rate can sustain at high level as shown in the scenario08-1-2 and 08-2-2.

6. CONCLUSIONS

In this study, the study area and grid geometry of the numerical model were revised from those of Sakagawa et al. (1994). Also the recharge rate, the conductive heat flux in the lower-most layer, and the permeability of the whole study area were adjusted. This numerical model was able to reproduce wells' initial temperature profile and pressure distribution in natural state modeling and was generally able to match the temperature history of feed points of production wells and reservoir pressure of observation wells in history matching.
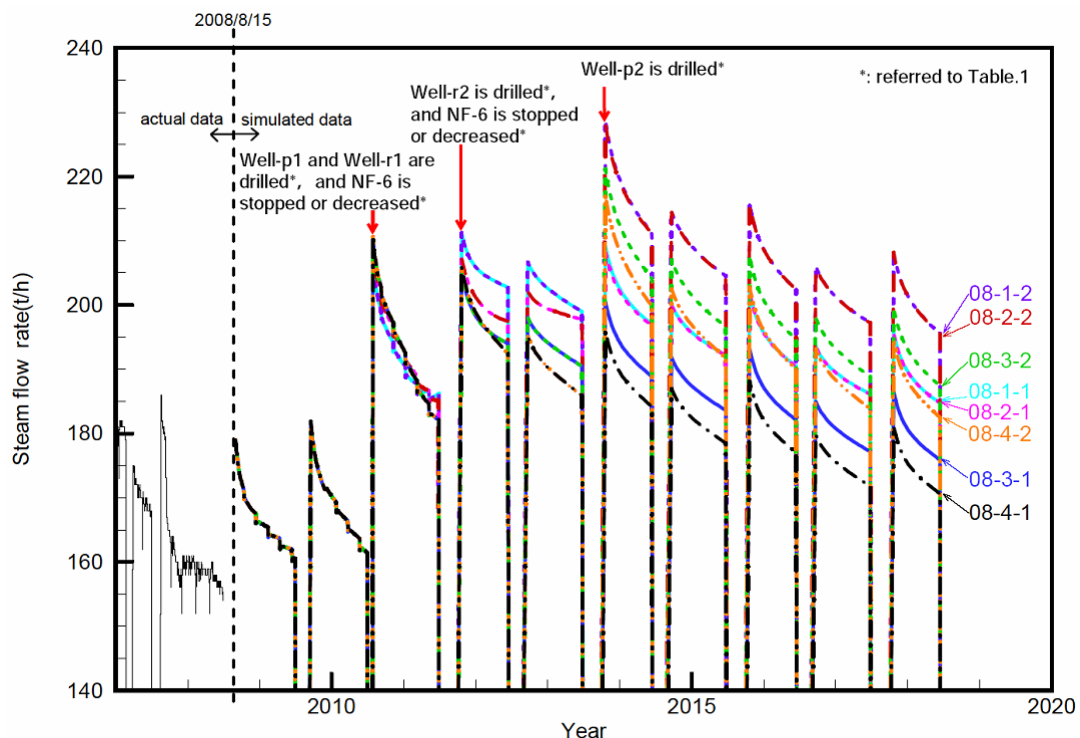
Figure 10: Result of prediction of steam flow rate.

Figure 11: Results of prediction of production rate in the production well ND-7 and NF-1 in scenario 08-1-1.

Using this numerical model, prediction of the future was carried out to obtain the appropriate assignment of production and re-injection. The results indicate that the reservoir will be able to sustain stable total steam production by drilling new production wells and simultaneously new re-injection wells. Because of drilling new re-injection wells, re-injection flow rate to the distant area from the caldera can be increased, and re-injection flow rate to the caldera wall can be decreased.

ACKNOWLEDGEMENT

REFERENCES

Akazawa, T., Kurozumi, H., Komatsu, R., and Demboya, N.: Characteristics of Fractures in the Mori Geothermal Field, Abstr. With Progr., Annual Meeting, Geothermal Research Society of Japan, **A7**, (1993) (in Japanese).

Ando, S., Kurozumi, H., and Komatsu, R.: Structure and Caldera-fill Deposits of Nigorikawa Caldera, Abstr., 29th International Geological Congress, **2**, (1992), 480.

Hanano, M., Kajiwara, T., Hishi, Y., Arai, F., Asanuma, M., Sato, K. and Takanohashi, M.: Overview of Production at the Mori Geothermal Field, Japan, Proc. World Geothermal Congress 2005, Antalya, (2005).

Kurozumi, H., and Doi, N.: Inner Structure of the Nigorikawa Caldera, Hokkaido, Japan, Bull. Volcano. Soc. Japan, **48(3),** (2003), 259-274. (in Japanese with English abstract).

Pritchett, J. W.: STAR: A geothermal reservoir simulation System, Proc. World Geothermal Congress 1995, Florence, (1995), 2959-2963.

Sato, K.: Mori Geothermal Power Plant, Geothermal Fields and Geothermal Power Plants in Japan, International Symposium on Geothermal Energy, Kumamoto and Beppu, Japan, (1988), 21-25.

Sakagawa, Y., Takahashi, M., Hanano, M., Ishido, T., and Demboya, N.: Numerical Simulation of the Mori Geothermal Field, Japan, Proceedings, Nineteenth Workshop on Geothermal Reservoir Engineering, Stanford University, Stanford, CA (1994), 171-178.

Sumi, K., and Takashima, I.: Absolute ages of the hydrothermal alteration halos associated volcanic rocks in some Japanese geothermal fields, "2nd U.N. Geothermal Symposium on the Development and Use of Geothermal Resources, (1975), 625-634.

Urakami, K., and Nishida, Y.: Heat Discharge Measurement and Geophysical Prospecting at Nigorikawa Basin, Northern Part of Komagatake, Bull. Geol. Surv. Japan, **28**, (1977), 1-20 (in Japanese with English abstract).